

# Resonant low-energy electron scattering on short-range impurities in graphene

D. M. Basko\*

*International School of Advanced Studies (SISSA), via Beirut 2-4, 34014 Trieste, Italy*

Resonant scattering of electrons with low energies (as compared to the bandwidth) on a single neutral short-range impurity in graphene is analyzed theoretically, taking into account the valley degeneracy. Resonances dramatically increase the scattering cross-section and introduce a strong energy dependence. Analysis of the tight-binding model shows that resonant scattering is typical for generic impurities as long as they are sufficiently strong (the potential is of the order of the electron bandwidth or higher).

## I. INTRODUCTION

Electron transport in graphene is a subject of intense study, both theoretical and experimental, since the very discovery of this material in 2004.<sup>1</sup> In general, electron transport is determined by competition of different scattering mechanisms, both inelastic (e. g., electron-phonon) and elastic (static defects). Elastic scattering is dominant at sufficiently low temperatures.

Different kinds of crystal imperfections can cause elastic electron scattering in graphene: mesoscopic corrugations of the graphene sheet (ripples)<sup>2</sup> producing perturbations smooth on the atomic scale, charged impurities producing long-range Coulomb fields, dislocations producing long-range strain fields, or short-range neutral impurities. While the first three types seem to be more important for the transport in the clean graphene, it is probably the fourth one that can be controlled. In Refs. 3,4 graphene oxide was chemically reduced to normal graphene; in Ref. 5 hydrogen and hydroxyl groups were deposited on the graphene sheet in a controlled and reversible manner; in all cases resistance changed by several orders of magnitude. Assuming that attachment of a chemical group to a carbon atom in graphene changes the hybridization of its electronic orbitals from  $sp^2$  to  $sp^3$ , one can view such group as a neutral short-range impurity.

Short-range impurities in carbon nanotubes have been studied even before the single-layer graphene was obtained in the laboratory.<sup>6,7,8,9,10</sup> Short-range impurities have been shown to modify local electronic properties of graphene, such as the local density of states<sup>11,12,13,14,15,16,17</sup> or local magnetic moment,<sup>13,18</sup> and to induce Friedel oscillations in doped samples.<sup>19</sup> The present work is dedicated to the problem of electron scattering on a single short-range impurity whose size  $R$  is assumed to be of the order of the interatomic distance  $a$  (the C-C bond length), and the electron energy  $\epsilon$  is assumed to be much smaller than the energy scale set by the potential,  $v/R$  ( $v$  is the electron velocity at the Dirac point, so that  $v/R$  is of the order of the electronic bandwidth). The main focus is the case of a strong impurity so that the results for electron scattering obtained in the first Born approximation<sup>20,21,22,23,24,25</sup> are not expected to be applicable. Instead, we are going to exploit the smallness  $|\epsilon|R/v \ll 1$ . For particles with

parabolic spectrum such low-energy scattering is characterized by a single constant of the dimensionality of length (the scattering length), determined from the solution of the Schrödinger equation at zero energy. In graphene, due to the degeneracy of the spectrum at the Dirac point, more than one length is needed to characterize a scatterer.<sup>26</sup>

The common intuition is that for a strong enough scatterer the typical value of scattering lengths  $l \sim R$ , yielding the cross-section  $\sigma \sim pl^2 \ll a$  (here  $p = |\epsilon|/v$  is the electron momentum counted from the Dirac point). The exception to this is the case of resonant scattering when the potential has a (quasi-)bound state with small energy, then one of the scattering lengths becomes of the order of the size of this state. The main motivation for the present study is that for the Dirac spectrum the exception becomes a rule: a vacancy (which can be viewed as the limit of an infinitely strong scatterer) introduces a bound state exactly at the Dirac point,<sup>11</sup> so one of the scattering lengths diverges. As a consequence, the scattering cross-section diverges as the electron energy approaches the Dirac point. This divergence corresponds to that found in the scattering off vacancies<sup>13,27</sup> and in the unitary limit of potential impurities.<sup>28</sup>

It is hard to introduce a real vacancy in graphene, however, if the  $\pi$ -orbital of some carbon atom is very tightly bound, this atom acts effectively as a vacancy for the rest of the  $\pi$ -electrons in the crystal. In particular, impurities introduced electrochemically<sup>3,4,5</sup> are likely to act as strong scatterers, and thus are unlikely to be described by the first Born approximation. This expectation is supported by density-functional theory (DFT) calculations for graphene<sup>29</sup> (a hypothetical material obtained from graphene by attaching a hydrogen atom to each carbon): the binding energy was obtained to be about 7 eV per hydrogen atom. For such scatterers the scattering length should be large, thus motivating the present study.

The main framework of this study is the general scattering theory<sup>30</sup> modified for the 2D Dirac equation<sup>31,32,33</sup> taking into account the valley degeneracy. In Sec. III we show that for a general short-range scatterer all the information necessary to determine the cross-section up to corrections of the order  $(pR)^2$  is encoded in a  $4 \times 4$  matrix  $L$  and a constant  $r_0$  (all having the dimensionality of length). The terms of the order  $(pR)^2$  and higher cannot be studied using the Dirac equation, as the Dirac hamil-

tonian itself is the leading term in the expansion of a microscopic hamiltonian in the parameter  $pa$  (and  $R \sim a$  is always assumed here). The matrix  $L$  (i) can be obtained from the solution of the microscopic Schrödinger equation (e. g., an *ab initio* calculation) for electrons in the graphene crystal at zero energy and with an appropriate asymptotics; (ii) is hermitian and invariant with respect to the time reversal, so it depends on 10 real parameters; (iii) its four eigenvalues  $l_1, \dots, l_4$  play the role of the scattering lengths. Divergence of one or several of these eigenvalues signals the existence of a localized solution at zero energy. For the parameter  $r_0$  we have (i)  $r_0 \sim R$ ; (ii) the dependence of the scattering amplitude on  $r_0$  is weak (logarithmic); (iii) the exact value of  $r_0$  cannot be extracted from the zero-energy solutions only, wave functions at low but finite energies have to be considered in order to determine it. When  $L$  and  $r_0$  are known, the low-energy scattering  $T$ -matrix is given by Eq. (19), which covers both Born limit [ $T(\epsilon)$  is  $\epsilon$ -independent, the cross-section  $\sigma \propto \epsilon$ ] and the unitary limit [ $T(\epsilon) \propto 1/(\epsilon \ln \epsilon)$ ,  $\sigma \propto 1/|\epsilon \ln^2 \epsilon|$ ], as well as the crossover between them for an impurity of a large but finite strength.

In Sec. IV we consider two examples of impurities with special symmetries, and see how these symmetries manifest themselves in the scattering (i. e., how they restrict the form of the matrix  $L$ ). The first example (the site-like impurity) is an impurity localized around one of the carbon atoms and preserving its  $C_{3v}$  symmetry ( $C_{3v}$  consists of three-fold rotations and reflections in three planes perpendicular to the crystal plane); it is natural to assume that this would be the case for a hydrogen atom bound to a carbon. The second kind (the bond-like impurity) involves two neighboring carbon atoms and the bond between them and has the symmetry  $C_{2v}$ . This could be the case for an oxygen atom bound to two carbon atoms. The two kinds of impurities, described above, are schematically shown in Fig. 1. Of course, a generic impurity is not going to have any symmetry at all.

Since graphene crystal is symmetric, impurities of the same kind can occur in different locations and with different orientations with equal probability, if these can be related to each other by a crystal symmetry operation. For example, the site-like impurity, located on an  $A$  atom in Fig. 1, can reside on a  $B$  atom with the same probability; the bond-like impurity can have one of the three different orientations, rotated by  $2\pi/3$  with respect to each other. Although equivalent from the crystal symmetry point of view, such impurities will have different  $L$  matrices. If one is not looking at effects of coherent scattering off several impurities, the cross-section can be averaged over such equally probable impurity configurations. This procedure is described in Sec. V.

In Sec. VI we perform explicit calculations in the tight-binding model as an example of microscopic model (i. e., well-defined at short distances), using the standard  $T$ -matrix approach on a lattice, adopted by many authors.<sup>12,13,14,15,16,17</sup> We consider the two kinds of im-

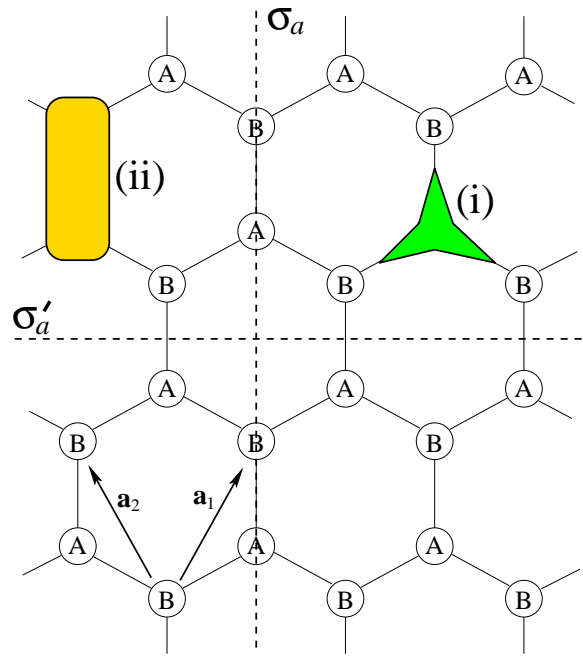


FIG. 1: (Color online). The honeycomb lattice with two atoms ( $A$  and  $B$ ) per unit cell and the elementary translation vectors  $\mathbf{a}_1$  and  $\mathbf{a}_2$ . The two inequivalent reflection planes  $\sigma_a$  and  $\sigma'_a$  are shown. (i) and (ii) are schematic representations of site-like and bond-like impurities with symmetries  $C_{3v}$  and  $C_{2v}$ , respectively.

purities, mentioned above, modeled as a diagonal on-site potential for a site-like impurity, and a combination of a diagonal and an off-diagonal potentials for a bond-like impurity (the same model was adopted in Ref. 15). The scattering lengths are calculated as functions of the impurity strengths, and  $r_0$  is obtained to be  $0.5a$ . In agreement with the results of Ref. 15, the divergence of the scattering length occurs at infinite impurity strength for a site-like impurity (corresponding to a zero-energy state bound to a vacancy), and at finite values of the diagonal and off-diagonal strengths for a bond-like impurity. The resulting cross-sections as functions of the electron energy for different impurity strengths are shown in Figs. 2,3.

## II. FREE ELECTRONS IN GRAPHENE

Graphene unit cell contains two atoms, labelled  $A$  and  $B$  (Fig. 1). Each of them has one  $\pi$ -orbital, so there are two electronic states for each point of the first Brillouin zone (the electron spin is not considered in the present work). The electronic energy  $\epsilon$  (measured from the Fermi level of the undoped graphene) vanishes at the two Dirac points  $K, K'$  with wave vectors  $\pm \mathbf{K}$ . Thus, there are exactly four electronic states with  $\epsilon = 0$ . An arbitrary linear combination of them is represented by a 4-component column vector  $\psi$ . Here we choose the fol-

$C_{6v}$	$E$	$C_2$	$2C_3$	$2C_6$	$\sigma_{a,b,c}$	$\sigma'_{a,b,c}$
$A_1$	1	1	1	1	1	1
$A_2$	1	1	1	1	-1	-1
$B_2$	1	-1	1	-1	1	-1
$B_1$	1	-1	1	-1	-1	1
$E_1$	2	-2	-1	1	0	0
$E_2$	2	2	-1	-1	0	0

TABLE I: Irreducible representations of the group  $C_{6v}$  and their characters.

irrep	$A_1$	$B_1$	$A_2$	$B_2$	$E_1$	$E_2$
valley-diagonal matrices						
matrix	$\mathbb{1}$	$\Lambda_z$	$\Sigma_z$	$\Sigma_z \Lambda_z$	$\Sigma_x, \Sigma_y$	$-\Sigma_y \Lambda_z, \Sigma_x \Lambda_z$
valley-off-diagonal matrices						
matrix	$\Sigma_z \Lambda_x$	$\Sigma_z \Lambda_y$	$\Lambda_x$	$\Lambda_y$	$\Sigma_y \Lambda_x, -\Sigma_x \Lambda_x$	$\Sigma_x \Lambda_y, \Sigma_y \Lambda_y$

TABLE II: Classification of  $4 \times 4$  hermitian matrices by irreducible representations of the  $C_{6v}$  group. Matrices joined by braces transform through each other under translations.

lowing arrangement of the wave function components in the column:<sup>26</sup>

$$\psi = \begin{bmatrix} \psi_{AK} \\ \psi_{BK} \\ \psi_{BK'} \\ -\psi_{AK'} \end{bmatrix}. \quad (1)$$

Other definitions of the column vector are possible, but they are inconvenient for the present problem; for the discussion see Appendix A and Ref. 34. Being interested in low-energy states, we focus on states in the vicinities of the Dirac points. The wave vectors of these states can be written as  $\mathbf{k} = \pm \mathbf{K} + \mathbf{p}$ , where  $pa \ll 1$  (here  $a \approx 1.42 \text{ \AA}$  is the C-C bond length). Equivalently, states near the Dirac points are obtained by including a smooth position dependence  $\psi(\mathbf{r})$ ,  $\mathbf{r} \equiv (x, y)$ .

The basis in the space of  $4 \times 4$  hermitian matrices is formed by 16 generators of the  $SU(4)$  group. They can be represented as products of two mutually commuting algebras of Pauli matrices denoted by  $\Sigma_x, \Sigma_y, \Sigma_z$  and  $\Lambda_x, \Lambda_y, \Lambda_z$ ,<sup>23,26</sup> which fixes their algebraic relations. We denote the unit  $4 \times 4$  matrix by  $\mathbb{1}$ , and sometimes  $\Sigma_0$  or  $\Lambda_0$  to make the formulas compact. In representation (1)  $\Sigma_i$  are the Pauli matrices acting within upper and lower 2-blocks (the sublattice subspace), while  $\Lambda_i$  are the Pauli matrices acting in the “external” subspace of the 2-blocks (the valley subspace). For 4-column vectors which can be represented as a direct product

$$\begin{bmatrix} x_1 y_1 \\ x_2 y_1 \\ x_1 y_2 \\ x_2 y_2 \end{bmatrix} \equiv \begin{bmatrix} x_1 \\ x_2 \end{bmatrix} \otimes \begin{bmatrix} y_1 \\ y_2 \end{bmatrix} \equiv \begin{bmatrix} x_1 \\ x_2 \end{bmatrix} \otimes (y_1 \phi_K + y_2 \phi_{K'}), \quad (2)$$

the  $\Sigma$  matrices act on the  $x$  variables, while the  $\Lambda$  matrices act on the  $y$  variables. The basis in the valley subspace is denoted by  $\phi_K, \phi_{K'}$  for future convenience.

The matrices  $\Sigma_i, \Lambda_j$ ,  $i, j = x, y, z$ , and their products have definite transformation properties under the crystal group. The irreducible representations of  $C_{6v}$  group are listed in Table I ( $C_n$  denotes the rotation by  $2\pi/n$ ,  $\sigma_{a,b,c}$  are the three reflections which swap the  $K$  and  $K'$  points,  $\sigma'_{a,b,c}$  are the three reflections which swap  $A$  and  $B$  atoms, the fixed point of these operations being the center of the hexagon, see Fig. 1). The correspondence between them and the matrices is given in Table II.<sup>35,36</sup>

The unitary matrices corresponding to the symmetry operations of the crystal can also be written in terms of  $\Sigma$  and  $\Lambda$  matrices, independently of the representation used.<sup>34</sup> Specifically,  $U_{C_3} = e^{(2\pi i/3)\Sigma_z}$  is the matrix of the  $C_3$  rotation,  $U_{C_2} = \Sigma_z \Lambda_x$  – of the  $C_2$  rotation,  $U_{\sigma'_a} = \Sigma_x \Lambda_z$  – of the  $\sigma'_a$  reflection,  $U_{\sigma_a} = \Sigma_y \Lambda_y$  – of the  $\sigma_a$  reflection. The two elementary translations by the vectors  $\mathbf{a}_1, \mathbf{a}_2$  act on the wave function as  $t_{\mathbf{a}_{1,2}} : \psi(\mathbf{r}) \mapsto e^{\mp(2\pi i/3)\Lambda_z} \psi(\mathbf{r} - \mathbf{a}_{1,2})$ . The time reversal operation is defined as  $\psi \mapsto U_t \psi^*$ , where the unitary time reversal matrix assumes the convenient form  $U_t = \Sigma_y \Lambda_y$  in representation (1).

Taking the leading-order term in the expansion of the band hamiltonian in the powers  $pa \ll 1$ , we describe the electrons by the Dirac hamiltonian

$$H_0 = -iv \boldsymbol{\Sigma} \cdot \nabla, \quad (3)$$

where  $\boldsymbol{\Sigma} = (\Sigma_x, \Sigma_y)$  is a two-dimensional vector, and  $v \approx 10^8 \text{ cm/s}$  is the electron velocity. The eigenstates of the Dirac hamiltonian with a definite value of momentum are plane waves:

$$\psi_{\mathbf{p}\mathbf{s}\kappa}^{(0)}(\mathbf{r}) = e^{i\mathbf{p}\mathbf{r}} \psi_{\varphi_{\mathbf{p}}\mathbf{s}\kappa}^{(0)}, \quad (4a)$$

$$\psi_{\varphi_{\mathbf{p}}\mathbf{s}\kappa}^{(0)} = \frac{1}{\sqrt{2}} \begin{bmatrix} s e^{-i\varphi/2} \\ e^{i\varphi/2} \end{bmatrix} \otimes \phi_{\kappa} = W_{\varphi}^{\dagger} \frac{1}{2} \begin{bmatrix} 1+s \\ 1-s \end{bmatrix} \otimes \phi_{\kappa}, \quad (4b)$$

with the energy  $\epsilon_{\mathbf{p}\mathbf{s}\kappa} = svp$ . The index  $s = \pm 1$  distinguishes between the conduction and the valence band. The unitary matrices  $W_{\varphi_{\mathbf{p}}} = e^{i\Sigma_y \pi/4} e^{i\Sigma_z \varphi_{\mathbf{p}}/2}$ , where  $\varphi_{\mathbf{p}} = \arctan(p_y/p_x)$  is the polar angle of the vector  $\mathbf{p}$ , diagonalize the Dirac hamiltonian in the momentum representation:  $v\mathbf{p} \cdot \boldsymbol{\Sigma} = W_{\varphi_{\mathbf{p}}}^{\dagger} v p \Sigma_z W_{\varphi_{\mathbf{p}}}$  (note that  $W_{\varphi=2\pi} = -W_{\varphi=0}$ ). The index  $\kappa = K, K'$  labels the valleys. As hamiltonian (3) does not contain  $\Lambda$  matrices, the valley subspace is degenerate, so any other basis can be chosen.

Besides plane waves, we will need the wave functions of states with a definite half-integer value of the “total angular momentum”  $j_z = -i(\partial/\partial\varphi) + (1/2)\Sigma_z$  which also commutes with the Dirac hamiltonian (3):

$$\psi_{p j_z \mathbf{s}\kappa}^{(0)}(\mathbf{r}) = \frac{1}{\sqrt{2}} \begin{bmatrix} s J_{j_z-1/2}(pr) e^{i(j_z-1/2)(\varphi+\pi/2)} \\ J_{j_z+1/2}(pr) e^{i(j_z+1/2)(\varphi+\pi/2)} \end{bmatrix} \otimes \phi_{\kappa}, \quad (5)$$

where  $J_m$  are Bessel functions of the first kind. If one relaxes the condition of regularity of the wave function at  $\mathbf{r} = 0$ , the Bessel functions of the first kind  $J_m$  can be

replaced by the Bessel functions of the second kind  $Y_m$ , or Hankel functions  $H_m^{(1,2)} = J_m \pm iY_m$ .

### III. RESONANT SCATTERING ON A SHORT-RANGE POTENTIAL

#### A. General definitions

Here we use the standard expansion in partial waves<sup>30</sup> modified for the Dirac equation analogously to Refs. 31,32,33. For a potential  $V(\mathbf{r})$  that falls off rapidly at distances  $r \gtrsim R$ , the electron motion at distances  $r \gg R$  can be considered free. The general scattering solution corresponding to the energy  $\epsilon = svp$  can be written as

$$\begin{aligned} \psi_{\mathbf{p}s\kappa}(\mathbf{r}) = & \sum_{m=-\infty}^{\infty} \frac{e^{-i(m+1/2)\varphi_{\mathbf{p}}}}{\sqrt{2}} \begin{bmatrix} sJ_m(pr)e^{im(\varphi+\pi/2)} \\ J_{m+1}(pr)e^{i(m+1)(\varphi+\pi/2)} \end{bmatrix} \otimes \phi_{\kappa} + \\ & + \sum_{m=-\infty}^{\infty} \frac{1}{\sqrt{2}} \begin{bmatrix} sH_m^{(1)}(pr)e^{im(\varphi+\pi/2)} \\ H_{m+1}^{(1)}(pr)e^{i(m+1)(\varphi+\pi/2)} \end{bmatrix} \otimes \frac{1}{2} \mathcal{F}_{m+1/2}^s(\mathbf{p})\phi_{\kappa}. \end{aligned} \quad (6)$$

The first sum represents just the incident plane wave (4). The second sum in Eq. (6) represents the outgoing scattered wave. Since a short-range potential can change arbitrarily the structure of the state in the valley subspace, an arbitrary  $2 \times 2$  matrix  $\mathcal{F}_{m+1/2}^s(\mathbf{p})$  is introduced (the factor  $1/2$  in front of  $\mathcal{F}$  is introduced for convenience).<sup>39</sup> The  $2 \times 2$  matrix  $\mathcal{F}$  can be represented as a linear combination of  $\Lambda$  matrices.

Using the asymptotic behaviour of  $H_m^{(1)}(pr)$  at  $pr \gg |m^2 - 1/4|$  for integer  $m$ :

$$H_m^{(1)}(pr) \underset{pr \rightarrow \infty}{\sim} \sqrt{\frac{2/\pi}{pr}} e^{ipr - im\pi/2 - i\pi/4}, \quad (7)$$

and the standard definitions of the scattering amplitude  $f_s(\varphi, \varphi_{\mathbf{p}}; p)$  and the scattering matrix  $\mathcal{S}_s(\varphi, \varphi'; p)$  in two dimensions,<sup>37</sup> where the existence of the degenerate valley subspace is taken into account:

$$\psi_{\mathbf{p}s\kappa}(\mathbf{r}) \underset{r \rightarrow \infty}{\sim} e^{i\mathbf{p}\mathbf{r}} \psi_{\varphi_{\mathbf{p}}s\kappa}^{(0)} + \frac{e^{ipr+i\pi/4}}{\sqrt{r}} f_s(\varphi_{\mathbf{r}}, \varphi_{\mathbf{p}}; p) \psi_{\varphi_{\mathbf{r}}s\kappa}^{(0)}, \quad (8a)$$

$$\psi_{\mathbf{p}s\kappa}(\mathbf{r}) \underset{r \rightarrow \infty}{\sim} \frac{e^{-ipr+i\pi/4}}{\sqrt{2\pi pr}} 2\pi\delta(\varphi_{\mathbf{r}} - \varphi_{\mathbf{p}} - \pi) \psi_{\varphi_{\mathbf{p}}s\kappa}^{(0)} + \frac{e^{ipr-i\pi/4}}{\sqrt{2\pi pr}} \mathcal{S}_s(\varphi_{\mathbf{r}}, \varphi_{\mathbf{p}}; p) \psi_{\varphi_{\mathbf{r}}s\kappa}^{(0)}, \quad (8b)$$

we relate them to the matrix  $\mathcal{F}_{m+1/2}^s(\mathbf{p})$ ; calculating the probability current  $\mathbf{j}(\mathbf{r}) = \psi^\dagger(\mathbf{r}) v \Sigma \psi(\mathbf{r})$ , we obtain the differential cross-section  $d\sigma_{s\kappa\kappa'}(\varphi, \varphi'; p)$  for an incident particle with momentum  $\mathbf{p} = (p \cos \varphi', p \sin \varphi')$  in the valley  $\kappa'$  to be scattered into the valley  $\kappa$  in the direction  $\mathbf{n} = (\cos \varphi, \sin \varphi)$ :

$$f_s(\varphi, \varphi'; p) = \frac{\mathcal{F}_s(\varphi, \varphi'; p)}{i\sqrt{2\pi p}}, \quad (9a)$$

$$\mathcal{S}_s(\varphi, \varphi'; p) = \mathbb{1}_{2 \times 2} 2\pi\delta(\varphi - \varphi') + \mathcal{F}_s(\varphi, \varphi'; p), \quad (9b)$$

$$\mathcal{F}_s(\varphi, \varphi_{\mathbf{p}}; p) \equiv \sum_{m=-\infty}^{\infty} \mathcal{F}_{m+1/2}^s(\mathbf{p}) e^{i(m+1/2)\varphi}, \quad (9c)$$

$$\frac{d\sigma_{s\kappa\kappa'}(\varphi, \varphi'; p)}{d\varphi} = |\phi_{\kappa}^\dagger f_s(\varphi, \varphi'; p) \phi_{\kappa'}|^2. \quad (9d)$$

Note that  $\psi_{\varphi+2\pi, s\kappa}^{(0)} = -\psi_{\varphi s\kappa}^{(0)}$ ; the above definitions imply  $0 \leq \varphi_{\mathbf{r}} - \varphi_{\mathbf{p}} < 2\pi$ . For  $-2\pi \leq \varphi_{\mathbf{r}} - \varphi_{\mathbf{p}} < 0$  we have to set  $\mathcal{S}_s(\varphi, \varphi'; p) = -\mathcal{S}_s(\varphi + 2\pi, \varphi'; p)$ . The scattering matrix satisfies the unitarity and reciprocity conditions (the latter assuming the symmetry of the scattering potential with respect to the time reversal):

$$\int_0^{2\pi} \frac{d\varphi}{2\pi} \mathcal{S}_s^\dagger(\varphi, \varphi_1; p) \mathcal{S}_s(\varphi, \varphi_2; p) = \mathbb{1}_{2 \times 2} 2\pi\delta(\varphi_1 - \varphi_2), \quad (10a)$$

$$\mathcal{S}_s(\varphi, \varphi'; p) = \Lambda_y \mathcal{S}_s^T(\varphi' + \pi, \varphi + \pi; p) \Lambda_y, \quad (10b)$$

where  $\mathcal{S}^T$  denotes the transpose of the matrix  $\mathcal{S}$ . The scattering amplitude can be related to the  $T$ -matrix  $T(\mathbf{p}, \mathbf{p}'; \epsilon)$  on the mass shell,  $|\mathbf{p}| = |\mathbf{p}'| = |\epsilon|/v$ . Starting from the exact expression for the scattered wave function,

$$\psi_{\mathbf{p}s\kappa}(\mathbf{r}) = e^{i\mathbf{p}\cdot\mathbf{r}}\psi_{\varphi\mathbf{p}s\kappa}^{(0)} + \int \frac{d^2\mathbf{p}'}{(2\pi)^2} e^{i\mathbf{p}'\cdot\mathbf{r}} G(\mathbf{p}', svp) T(\mathbf{p}', \mathbf{p}; svp) \psi_{\varphi\mathbf{p}s\kappa}^{(0)}, \quad G(\mathbf{p}, \epsilon) \equiv \frac{\epsilon \mathbf{1} + v\mathbf{p} \cdot \boldsymbol{\Sigma}}{\epsilon^2 - (vp - i0^+)^2}, \quad (11)$$

and taking its  $pr \gg 1$  asymptotics, we arrive at  $[\mathbf{n} = (\cos \varphi, \sin \varphi)$  and  $\mathbf{n}' = (\cos \varphi', \sin \varphi')$  are unit vectors]:

$$W_\varphi T(p\mathbf{n}, p\mathbf{n}'; svp) W_{\varphi'}^\dagger = \frac{iv}{p} \frac{1}{2} \begin{bmatrix} 1+s & 0 \\ 0 & 1-s \end{bmatrix} \otimes s\mathcal{F}^s(\varphi, \varphi'; p). \quad (12)$$

## B. Scattering lengths

At  $r \sim R$  the potential mixes different terms in Eq. (6). The asymptotic behaviour of the Bessel and Hankel functions at  $pr \ll \sqrt{|m|+1}$  for integer  $m$  is given by

$$J_m(pr) = \frac{(\text{sign } m)^m}{|m|!} \left(\frac{pr}{2}\right)^{|m|}, \quad (13a)$$

$$H_{m \neq 0}^{(1)}(pr) = \frac{(\text{sign } m)^m |m|!}{i\pi |m|} \left(\frac{2}{pr}\right)^{|m|}, \quad (13b)$$

$$H_0^{(1)}(pr) = 1 + \frac{2i}{\pi} \left(\ln \frac{pr}{2} + \gamma\right), \quad (13c)$$

where  $\gamma = 0.5772\dots$  is the Euler-Mascheroni constant. At this stage we make an assumption that all terms constituting the scattered wave in Eq. (6) should be of the same order at  $r \sim R$ , provided that *their coupling is allowed by the symmetry of the scattering potential*. Depending on the symmetry of the scattering potential, we have to consider two cases. (i) The potential is isotropic and  $\Sigma_z$ -conserving:  $V(\mathbf{r}) = V(r)$ ,  $\Sigma_z V(\mathbf{r}) \Sigma_z = V(\mathbf{r})$  (this case was analyzed in Refs. 31,32,33). Then  $j_z = -i(\partial/\partial\varphi) + (1/2)\Sigma_z$  is conserved, so the terms in Eq. (6) with different values of  $m$  are decoupled (each term with a given  $m$  corresponds to  $j_z = m+1/2$ ). Matching the terms gives  $\mathcal{F}_{j_z} \sim (pR)^{2|j_z|}$ . (ii) The potential  $V(\mathbf{r})$  is generic, so it mixes all states with different values of  $j_z$ . Matching the terms gives  $\mathcal{F}_{j_z} \sim (pR)^{|j_z|+1/2}$ . Thus,  $\mathcal{F}_{\pm 1/2}$  are the most important terms in both cases; moreover, as typically  $R \sim a$ , considering the terms with  $|j_z| > 1/2$  would require going beyond the Dirac hamiltonian, since the Dirac hamiltonian itself is the leading term in the expansion in  $pa$ .

At  $r \ll 1/p$  we can neglect the energy in the Dirac equation, which becomes

$$[-iv\boldsymbol{\Sigma} \cdot \nabla + V(\mathbf{r})]\psi(\mathbf{r}) = 0. \quad (14)$$

At  $r \gg R$  this equation admits solutions of the form

$$r^m e^{im\varphi} \begin{bmatrix} 1 \\ 0 \end{bmatrix} \otimes \phi_\kappa, \quad r^{-m} e^{im\varphi} \begin{bmatrix} 0 \\ 1 \end{bmatrix} \otimes \phi_\kappa, \quad (15)$$

which determine the asymptotics of different angular harmonics of the *four* linearly independent zero-energy solutions. Since non-zero angular harmonics of the incident wave in Eq. (6) vanish at  $p \rightarrow 0$ , we are interested in the solutions of Eq. (14) whose asymptotics can be written as

$$\psi_{01v}(\mathbf{r}) \underset{r \rightarrow \infty}{\sim} \begin{bmatrix} 1 \\ 0 \end{bmatrix} \otimes \phi_\kappa + \frac{e^{i\varphi}}{ir} \begin{bmatrix} 0 \\ 1 \end{bmatrix} \otimes L_{11}\phi_\kappa + \frac{e^{-i\varphi}}{ir} \begin{bmatrix} 1 \\ 0 \end{bmatrix} \otimes L_{21}\phi_\kappa + \sum_{m>1} O\left(\frac{e^{\pm im\varphi}}{r^m}\right), \quad (16a)$$

$$\psi_{02v}(\mathbf{r}) \underset{r \rightarrow \infty}{\sim} \begin{bmatrix} 0 \\ 1 \end{bmatrix} \otimes \phi_\kappa + \frac{e^{i\varphi}}{ir} \begin{bmatrix} 0 \\ 1 \end{bmatrix} \otimes L_{12}\phi_\kappa + \frac{e^{-i\varphi}}{ir} \begin{bmatrix} 1 \\ 0 \end{bmatrix} \otimes L_{22}\phi_\kappa + \sum_{m>1} O\left(\frac{e^{\pm im\varphi}}{r^m}\right), \quad (16b)$$

where each  $L_{ij}$  is a  $2 \times 2$  matrix in the valley subspace, which has to be determined from the solution of the Schrödinger equation at short distances (the factor  $1/i$  is introduced for convenience). Let us associate the indices  $i, j = 1, 2$  of the  $2 \times 2$  matrices  $L_{ij}$  with the matrix sturcture in the  $\Sigma$ -subspace, thus combining the four  $2 \times 2$  matrices  $L_{ij}$  into a single  $4 \times 4$  matrix  $L$ . Then the asymptotic behavior of any solution of Eq. (14) at  $r \rightarrow \infty$  can be written as:

$$\psi(\mathbf{r}) = \psi^{(0)} + \frac{1}{ir} (\mathbf{n} \cdot \boldsymbol{\Sigma}) L \psi^{(0)} + \sum_{m>1} O\left(\frac{e^{\pm im\varphi}}{r^m}\right), \quad (17)$$

where  $\psi^{(0)}$  is an arbitrary 4-column. This equation could also be viewed as the boundary condition on the angular harmonics of the scattering solution (6) at  $r \rightarrow 0$ ; being formed at short distances  $r \sim R$ , this boundary condition should not depend on  $\epsilon$  for  $|\epsilon| \ll v/R$ . However, due to the logarithmic divergence of Hankel function  $H_0^{(1)}(pr)$ , matching of wave functions should be performed at some  $r = r_0 \sim R$ . Note that in contrast to the two-dimensional Schrödinger equation, the value of the constant  $r_0$  cannot be determined from the zero-energy solution since the logarithmic function is not a solution of the Dirac equation at zero energy.

Comparing expressions (16) to the scattering solution (6) and using asymptotic expressions (13), we obtain the general possible form of  $\mathcal{F}_{\pm 1/2}^s(\mathbf{p})$ :

$$\frac{i}{\pi p} \mathcal{F}_{+1/2}^s(\mathbf{p}) = sL_{11} \left[ e^{-i\varphi_{\mathbf{p}}/2} + \frac{1}{2} H_0^{(1)}(pr_0) \mathcal{F}_{+1/2}^s(\mathbf{p}) \right] + L_{12} \left[ e^{i\varphi_{\mathbf{p}}/2} + \frac{1}{2} H_0^{(1)}(pr_0) \mathcal{F}_{-1/2}^s(\mathbf{p}) \right], \quad (18a)$$

$$\frac{i}{\pi p} \mathcal{F}_{-1/2}^s(\mathbf{p}) = L_{21} \left[ e^{-i\varphi_{\mathbf{p}}/2} + \frac{1}{2} H_0^{(1)}(pr_0) \mathcal{F}_{+1/2}^s(\mathbf{p}) \right] + sL_{22} \left[ e^{i\varphi_{\mathbf{p}}/2} + \frac{1}{2} H_0^{(1)}(pr_0) \mathcal{F}_{-1/2}^s(\mathbf{p}) \right]. \quad (18b)$$

Solving these equations and comparing the result to Eq. (12), we obtain the general low-energy  $T$ -matrix:<sup>40</sup>

$$T(\epsilon) = \left[ \mathbb{1} + \frac{\epsilon}{v} \left( \ln \frac{2v}{r_0|\epsilon|} - \gamma + \frac{i\pi}{2} \right) L \right]^{-1} 2\pi v L, \quad (19)$$

which determines the differential cross-section:

$$\frac{d\sigma_{s\kappa\kappa'}(\varphi, \varphi'; p)}{d\varphi} = \frac{p}{2\pi v^2} \left| (\psi_{\varphi s\kappa}^{(0)})^\dagger T(svp) \psi_{\varphi' s\kappa'}^{(0)} \right|^2. \quad (20)$$

The matrix  $L$  satisfies (i)  $L = L^\dagger$  to ensure the unitarity of the scattering matrix (10a), and (ii)  $L = U_t L^T U_t^\dagger$  as a consequence of the reciprocity condition (10b). Thus, it has four orthogonal eigenvectors  $\psi_i$ :  $L\psi_i = l_i\psi_i$ ,  $i = 1, \dots, 4$ , and the four eigenvalues  $l_i$  play the role of the scattering lengths. The angular dependence of  $d\sigma_{s\kappa\kappa'}(\varphi, \varphi'; p)/d\varphi$  is given by the sum of an isotropic term and terms  $\propto e^{\pm i\varphi}, e^{\pm i\varphi'}$ , and  $e^{\pm i\varphi \pm i\varphi'}$  (with all four combinations of the signs). The total out-scattering cross-section (i. e., integrated over  $\varphi$  and summed over  $v$ ) takes the simple form:

$$\sigma_{s\kappa\kappa'}^{\text{out}}(\varphi'; p) = \sum_{i=1}^4 \frac{2\pi^2 p |\psi_i^\dagger \psi_{\varphi' s\kappa'}^{(0)}|^2}{[l_i^{-1} - sp \ln(e\gamma pr_0/2)]^2 + (\pi p/2)^2}. \quad (21)$$

Typically, one assumes that for a strong potential all scattering lengths  $l_i \sim R$ . However, an explicit calculation for a point defect in the tight-binding model, performed in Sec. VI, shows that one of the lengths  $l_i$  (let it be  $l_1$  for definiteness) can become arbitrarily large. The case  $l_1 \rightarrow \infty$  corresponds to the existence of a localized solution  $\psi(\mathbf{r}) \sim (\mathbf{n} \cdot \boldsymbol{\Sigma})\psi_1/r$  at zero energy.<sup>11</sup> In this case the cross-section diverges at  $p \rightarrow 0$ . This divergence corresponds to a similar divergence in the imaginary part of the electron self-energy found in Refs. 13,28; a similar divergence in the cross-section was found in Ref. 27. Note that even in the case of resonant scattering the scaling  $\mathcal{F}_{jz} \sim (pR)^{|jz|} \mathcal{F}_{\pm 1/2}$  holds: indeed, at  $l_1 \rightarrow \infty$  the coefficients at the  $1/r^m$  terms in the wave function of the localized state should scale as  $R^m$ , as there is no other length scale in the problem.

#### IV. IMPURITIES WITH SPECIAL SYMMETRIES

Let us consider two particular kinds of impurities, shown in Fig. 1.

(i) A site-like impurity with the symmetry  $C_{3v}$  whose fixed point is located on one of the atoms (let us assume it to be an  $A$  atom). Thus, the matrix  $L$  should be invariant under the reflection  $\sigma_a$  and the rotation  $C'_3 = C_3 t_{\mathbf{a}_1}$  (we remind that the rotation  $C_3$  is around the center of the hexagon). The conditions  $L = U_{\sigma_a}^\dagger L U_{\sigma_a}$ ,  $L = U_{C'_3}^\dagger L U_{C'_3}$  together with the time-reversal symmetry restrict the matrix  $L$  to

$$L = L_{A_1} \mathbb{1} + L_{B_2} \Lambda_z \Sigma_z + \tilde{L}_E (\Lambda_x \Sigma_x - \Lambda_y \Sigma_y). \quad (22)$$

The eigenvalues and eigenvectors of this family of matrices are

$$l_{1,2} = L_{A_1} + L_{B_2} \pm 2\tilde{L}_E, \quad l_{3,4} = L_{A_1} - L_{B_2} \quad (23a)$$

$$\psi_{1,2} = \frac{1}{\sqrt{2}} \begin{bmatrix} 1 \\ 0 \\ 0 \\ \pm 1 \end{bmatrix}, \quad \psi_{3,4} = \frac{1}{\sqrt{2}} \begin{bmatrix} 0 \\ 1 \\ \pm 1 \\ 0 \end{bmatrix}. \quad (23b)$$

The  $T$ -matrix has the same transformation properties as the matrix  $L$ , so it can be written in the same form (22) with the substitution  $L \rightarrow T$ . Then, according to Eq. (20) the differential intravalley and intervalley cross-sections can be written as

$$\frac{d\sigma_{KK}}{d\varphi} = \frac{p}{2\pi v^2} \left| T_{A_1} \cos \frac{\varphi - \varphi'}{2} + iT_{B_2} \sin \frac{\varphi - \varphi'}{2} \right|^2, \quad (24a)$$

$$\frac{d\sigma_{K'K}}{d\varphi} = \frac{p}{2\pi v^2} |\tilde{T}_E|^2. \quad (24b)$$

(ii) A bond-like impurity with the symmetry  $C_{2v}$  whose fixed point is located at the center of a bond (let us assume it to be a bond connecting the two atoms within the same unit cell). Then, the matrix  $L$  should be invariant

under the reflection  $\sigma'_a$  and the rotation  $C'_2 = C_2 t_{\mathbf{a}_1} t_{\mathbf{a}_2}$ , which fixes

$$L = L_{A_1} \mathbb{1} + L_{E_2} \Lambda_z \Sigma_x + \tilde{L}_{A_1} \Lambda_x \Sigma_z + \tilde{L}_{E_2} \Lambda_y \Sigma_y, \quad (25a)$$

$$l_{1,2} = (L_{A_1} + \tilde{L}_{E_2}) \pm (L_{E_2} + \tilde{L}_{A_1}), \quad (25b)$$

$$l_{3,4} = (L_{A_1} - \tilde{L}_{E_2}) \pm (L_{E_2} - \tilde{L}_{A_1}), \quad (25c)$$

$$\psi_{1,2} = \frac{1}{2} \begin{bmatrix} \pm 1 \\ 1 \\ 1 \\ \mp 1 \end{bmatrix}, \quad \psi_{3,4} = \frac{1}{2} \begin{bmatrix} 1 \\ \pm 1 \\ \mp 1 \\ 1 \end{bmatrix}. \quad (25d)$$

The differential intravalley and intervalley cross-sections are

$$\frac{d\sigma_{KK}}{d\varphi} = \frac{p}{2\pi v^2} \left| T_{A_1} \cos \frac{\varphi - \varphi'}{2} + s T_{E_2} \cos \frac{\varphi + \varphi'}{2} \right|^2, \quad (26a)$$

$$\frac{d\sigma_{K'K}}{d\varphi} = \frac{p}{2\pi v^2} \left| \tilde{T}_{A_1} \sin \frac{\varphi - \varphi'}{2} + s \tilde{T}_{E_2} \sin \frac{\varphi + \varphi'}{2} \right|^2. \quad (26b)$$

If the location of the impurity is different from what we have assumed, its  $L$  matrix can be obtained by applying the corresponding symmetry operation. For example, in case (i) the matrix for an impurity located on a  $B$  atom is obtained by a  $C_2$  rotation:  $L \rightarrow \Lambda_x \Sigma_z L \Lambda_x \Sigma_z$ . Obviously, these two locations can occur with equal probability, so one could average over them. This procedure is described in the next section.

## V. AVERAGING OVER THE IMPURITIES

As discussed in the end of the preceding section, the presence of defects characterized by a certain  $T$ -matrix  $T(\mathbf{p}, \mathbf{p}', \epsilon)$  implies the presence of the same (on average) number of defects of the same type, placed in different locations with different orientations, and thus having different  $T$ -matrices, but equivalent with respect to the symmetry of the crystal. If one studies effects which do not involve coherent scattering on several impurities, it is sufficient to average any observable  $\mathcal{O}[T(\mathbf{p}, \mathbf{p}', \epsilon)]$ , calculated for a single impurity, according to

$$\begin{aligned} \overline{\mathcal{O}} = \frac{1}{3|C_{6v}|} \sum_{R \in C_{6v}} & \left( \mathcal{O}[U_R T(R\mathbf{p}, R\mathbf{p}', \epsilon) U_R^\dagger] + \right. \\ & + \mathcal{O}[U_{t_{\mathbf{a}_1}} U_R T(R\mathbf{p}, R\mathbf{p}', \epsilon) U_R^\dagger U_{t_{\mathbf{a}_1}}^\dagger] + \\ & \left. + \mathcal{O}[U_{t_{\mathbf{a}_1}}^\dagger U_R T(R\mathbf{p}, R\mathbf{p}', \epsilon) U_R^\dagger U_{t_{\mathbf{a}_1}}] \right). \quad (27) \end{aligned}$$

Here  $|C_{6v}| = 12$  is the number of elements in the  $C_{6v}$  group,  $R$  are the operations from the group, and  $U_R$  are their  $4 \times 4$  matrices in the  $\psi$ -representation. The averaging is performed also over the elementary translations with the matrices  $U_{t_{\mathbf{a}_1}} = e^{-(2\pi i/3)\Lambda_z}$  and  $U_{t_{\mathbf{a}_2}} = U_{t_{\mathbf{a}_1}}^\dagger$ . It is convenient to consider the group  $C''_{6v}$  – the direct product of the point group  $C_{6v}$  and the 3-cyclic group represented by the matrices  $\mathbb{1}, e^{\pm(2\pi i/3)\Lambda_z}$ . Then Eq. (27) describes simply the average over the group  $C''_{6v}$ .

Let us apply this procedure to the differential cross-section. We write the averaged Eq. (20) as

$$\frac{\overline{d\sigma}}{d\varphi} = \frac{p}{2\pi v^2} \sum_{R \in C''_{6v}} \frac{\text{Tr}\{U_R^\dagger (\psi' \psi'^\dagger) U_R T^\dagger U_R^\dagger (\psi \psi^\dagger) U_R T\}}{|C''_{6v}|}, \quad (28)$$

where we abbreviated  $\psi = \psi_{\varphi s\kappa}^{(0)}$ ,  $\psi' = \psi_{\varphi' s\kappa'}^{(0)}$ , and  $T = T(svp)$ . Thus, equivalently, we can calculate the average  $(\psi' \psi'^\dagger) \otimes (\psi \psi^\dagger)$ . In the matrices  $\psi \psi^\dagger$  and  $\psi' \psi'^\dagger$  we separate the components corresponding to different irreducible representations of  $C_{6v}$ :

$$\begin{aligned} \psi \psi^\dagger &= \frac{1}{4} \sum_{i,j=0,x,y,z} (\psi^\dagger \Lambda_i \Sigma_j \psi) \Lambda_i \Sigma_j = \\ &= \frac{1}{4} (\mathbb{1} \pm \Lambda_z)(\mathbb{1} + \mathbf{s}\mathbf{n} \cdot \boldsymbol{\Sigma}), \quad (29) \end{aligned}$$

where the plus (minus) sign should be taken for  $\phi_\kappa = \phi_K$  ( $\phi_\kappa = \phi_{K'}$ ), and  $\mathbf{n} = (\cos \varphi, \sin \varphi)$ . Let us label the matrices  $\Lambda_i \Sigma_j$  belonging to an irreducible representation  $r$  of the dimensionality  $d_r$  as  $(\Lambda \Sigma)_\ell^r$ , where the index  $\ell = 1, \dots, d_r$  labels the matrices within the representation. Then in each representation we can define the  $d_r \times d_r$  matrices  $(U_R^r)_{\ell\ell'}$  as

$$U_R^\dagger (\Lambda \Sigma)_\ell^r U_R = \sum_{\ell'=1}^{d_r} (U_R^r)_{\ell\ell'} (\Lambda \Sigma)_{\ell'}^r. \quad (30)$$

From the orthogonality relation for the representation matrices<sup>38</sup>

$$\frac{1}{|C_{6v}|} \sum_{R \in C_{6v}} (U_R^r)^*_{\ell_1 \ell_2} (U_R^r)_{\ell_3 \ell_4} = \frac{\delta_{r r'}}{d_r} \delta_{\ell_1 \ell_3} \delta_{\ell_2 \ell_4}, \quad (31)$$

we obtain the general expression:

$$\frac{d\sigma_{s\kappa\kappa'}(\varphi, \varphi'; p)}{d\varphi} = \frac{p}{32\pi v^2} \left[ \text{Tr} \{ \Lambda_0 T^\dagger(svp) \Lambda_0 T(svp) \} + \frac{1}{2} \cos(\varphi - \varphi') \sum_{j=x,y} \text{Tr} \{ \Lambda_0 \Sigma_j T^\dagger(svp) \Lambda_0 \Sigma_j T(svp) \} \right] + (2\delta_{\kappa\kappa'} - 1) [\Lambda_0 \rightarrow \Lambda_z]. \quad (32)$$

(here we denoted the  $4 \times 4$  unit matrix  $\mathbb{1}$  by  $\Lambda_0$ ).

To conclude this section, we note that the averaging procedure described above is equivalent to averaging the cross-section  $d\sigma(\varphi, \varphi')/d\varphi$  over  $(\varphi + \varphi')/2$  keeping  $\varphi - \varphi'$  fixed (due to the symmetry of the crystal with respect to  $C_3$  rotations), and subsequent averaging over the sign of  $\varphi - \varphi'$  (due to the symmetry with respect to reflections).

## VI. IMPURITIES IN THE TIGHT-BINDING MODEL

### A. Green's function

Let us consider the tight-binding model with nearest-neighbor coupling as an exactly solvable example of a microscopic model (i. e., well-defined at short distances). The only parameter of the clean hamiltonian is the nearest-neighbor matrix element which we write as  $-2v/(3a)$ , thus expressing it in terms of the electron velocity at the Dirac point. It is convenient to work with a 2-component wave function  $\{\Psi_A(\mathbf{r}_n), \Psi_B(\mathbf{r}_n)\}$  (corresponding to the two atoms in the unit cell), where the position of the unit cell  $\mathbf{r}_n = n_1 \mathbf{a}_1 + n_2 \mathbf{a}_2$  is labelled by two integers  $n_1, n_2$ . The tight-binding hamiltonian  $\mathcal{H}_0(\mathbf{r}_n - \mathbf{r}_{n'})$  is a  $2 \times 2$  matrix in the sublattice space.

The scattering problem in the tight-binding model with a few-site potential  $\mathcal{U}$  is conveniently solved using Lippmann-Schwinger equation:

$$\Psi = \Psi^{(0)} + \mathcal{G}(\epsilon) \mathcal{U} \Psi, \quad (33)$$

where  $\Psi^{(0)}$  is the incident wave,  $\Psi$  is the sought wave function, and  $\mathcal{G}(\epsilon) = (\epsilon - \mathcal{H}_0)^{-1}$  is the Green's function, explicitly given by

$$\mathcal{G}(\mathbf{r}_n - \mathbf{r}_{n'}, \epsilon) = \int \frac{d^2 \mathbf{k}}{A_{BZ}} \frac{e^{i\mathbf{k}(\mathbf{r}_n - \mathbf{r}_{n'})}}{\epsilon^2 - |t_{\mathbf{k}}|^2} \begin{pmatrix} \epsilon & -t_{\mathbf{k}} \\ -t_{\mathbf{k}}^* & \epsilon \end{pmatrix}, \quad (34)$$

$$t_{\mathbf{k}} = \frac{2v}{3a} (1 + e^{-i\mathbf{k}\mathbf{a}_1} + e^{-i\mathbf{k}\mathbf{a}_2}),$$

$$A_{BZ} \equiv \frac{(2\pi)^2}{A_{\text{uc}}} = \frac{(2\pi)^2}{\sqrt{27}a^2/2}.$$

The large-distance behavior of  $\mathcal{G}(\mathbf{r}, \epsilon)$  is determined by the singularities of the denominator, i. e., vicinities of the Dirac points  $\pm \mathbf{K}$ ,  $\mathbf{k} = \pm \mathbf{K} + \mathbf{p}$ , where we can approximate

$$1 + e^{-i(\pm \mathbf{K} + \mathbf{p})\mathbf{a}_1} + e^{-i(\pm \mathbf{K} + \mathbf{p})\mathbf{a}_2} \approx \frac{3a}{2} (\mp p_x + ip_y). \quad (35)$$

Focusing at  $|\epsilon| \ll v/a$ , we obtain for  $r \gg a$  (c. c. stands for the complex conjugate):

$$\mathcal{G}_{AA}(\mathbf{r}, \epsilon) = \frac{A_{\text{uc}}|\epsilon|}{4iv^2} (e^{i\mathbf{K}\mathbf{r}} + e^{-i\mathbf{K}\mathbf{r}}) sH_0^{(1)}(|\epsilon|r/v), \quad (36a)$$

$$\mathcal{G}_{BA}(\mathbf{r}, \epsilon) = \frac{A_{\text{uc}}|\epsilon|}{4iv^2} (e^{i\mathbf{K}\mathbf{r} + i\varphi + i\pi/2} + \text{c. c.}) H_1^{(1)}(|\epsilon|r/v), \quad (36b)$$

$$\mathcal{G}_{BA}(\mathbf{r}, 0) = \frac{A_{\text{uc}}}{v} \frac{e^{i\mathbf{K}\mathbf{r} + i\varphi} - e^{-i\mathbf{K}\mathbf{r} - i\varphi}}{2\pi i r}. \quad (36c)$$

We also need the Green's function at coinciding points:

$$\mathcal{G}_{AA}(\mathbf{0}, \epsilon) = -\frac{A_{\text{uc}}\epsilon}{\pi v^2} \left( \ln \frac{2v}{|\epsilon|r_0} - \gamma + \frac{i\pi}{2} \right) + O(\epsilon^3), \quad (37a)$$

$$\mathcal{G}_{BA}(\mathbf{0}, \epsilon) = \frac{a}{2v} + O(\epsilon^2). \quad (37b)$$

The value of  $r_0$  in Eq. (37a) is determined by the integration over the whole first Brillouin zone; numerical integration gives  $e^\gamma r_0 = a$  within the numerical precision. The leading term in Eq. (37b) can be easily obtained in the coordinate representation using the fact that  $\mathcal{H}_0^{-1}$ , just like  $\mathcal{H}_0$ , is invariant under  $C_3$  rotations around each carbon atom.

### B. One-site impurity

Let us add the on-site potential  $U_0$  different from zero only on the  $A$  atom of the  $n_1 = n_2 = 0$  unit cell. The limit  $U_0 \rightarrow \infty$  is equivalent to imposing the boundary condition  $\Psi_A(\mathbf{0}) = 0$  and thus describes a vacancy.

First of all, we note that the two plane wave states with  $\Psi_A(\mathbf{r}_n) = 0$ ,  $\Psi_B(\mathbf{r}_n) = e^{\pm i\mathbf{K}\mathbf{r}_n}$  remain the zero-energy eigenstates of the hamiltonian even in the presence of the potential. In the representation (1) these two states are represented by the 4-columns

$$\begin{bmatrix} 0 \\ 1 \\ 0 \\ 0 \end{bmatrix} = \begin{bmatrix} 0 \\ 1 \end{bmatrix} \otimes \phi_K, \quad \begin{bmatrix} 0 \\ 0 \\ 1 \\ 0 \end{bmatrix} = \begin{bmatrix} 1 \\ 0 \end{bmatrix} \otimes \phi_{K'}.$$

Comparing them to the asymptotic forms (16), we see that  $L_{11}\phi_{K'} = L_{21}\phi_{K'} = 0$ ,  $L_{12}\phi_K = L_{22}\phi_K = 0$ .



The other two zero-energy solutions correspond to the incident wave on the  $A$ -sublattice,  $\Psi_A^{(0)}(\mathbf{r}_n) = e^{\pm i\mathbf{K}\mathbf{r}_n}$ ,  $\Psi_B^{(0)}(\mathbf{r}_n) = 0$ . In the representation (1) these two states are represented by the 4-columns

$$\begin{bmatrix} 1 \\ 0 \\ 0 \\ 0 \end{bmatrix} = \begin{bmatrix} 1 \\ 0 \end{bmatrix} \otimes \phi_K, \quad \begin{bmatrix} 0 \\ 0 \\ 0 \\ -1 \end{bmatrix} = \begin{bmatrix} 0 \\ -1 \end{bmatrix} \otimes \phi_{K'}.$$

As the potential  $U_0$  is localized on one atom, and  $\mathcal{G}(\epsilon = 0)$  is off-diagonal in the sublattices, the Lippmann-Schwinger equation is straightforwardly solved to give the wave function:

$$\Psi_A(\mathbf{r}_n) = e^{\pm i\mathbf{K}\mathbf{r}_n}, \quad \Psi_B(\mathbf{r}_n) = U_0 \mathcal{G}_{BA}(\mathbf{r}_n, \epsilon = 0). \quad (38)$$

Using Eq. (36c), we obtain

$$L = \frac{A_{uc}U_0}{\pi v} \frac{\mathbb{1} + \Lambda_z \Sigma_z + \Lambda_y \Sigma_y - \Lambda_x \Sigma_x}{4}, \quad (39)$$

in agreement with Eq. (22). The eigenvalues of this matrix are easily found to be  $l_1 = A_{uc}U_0/(\pi v)$ ,  $l_2 = l_3 = l_4 = 0$ . At  $U_0 \rightarrow \infty$  the scattering length  $l_1$  diverges. In this case the amplitude of the incident wave can be set to zero, and  $\Psi_B(\mathbf{r}_n) \propto \mathcal{G}_{BA}(\mathbf{r}, \epsilon = 0)$  is the wave function of the state, localized on the vacancy.

At  $\epsilon \neq 0$  the Lippmann-Schwinger equation is solved self-consistently for  $\Psi_A(\mathbf{0})$  to give the wave functions:

$$\begin{aligned} \Psi_{\mathbf{k}s}(\mathbf{r}_n) = & \begin{pmatrix} e^{i\Phi_{\mathbf{k}}/2} \\ -se^{-i\Phi_{\mathbf{k}}/2} \end{pmatrix} \frac{e^{i\mathbf{k}\mathbf{r}_n}}{\sqrt{2}} + \\ & + \frac{e^{i\Phi_{\mathbf{k}}/2}/\sqrt{2}}{U_0^{-1} - \mathcal{G}_{AA}(\mathbf{0}, \epsilon)} \begin{pmatrix} \mathcal{G}_{AA}(\mathbf{r}_n, \epsilon) \\ \mathcal{G}_{BA}(\mathbf{r}_n, \epsilon) \end{pmatrix} \end{aligned} \quad (40)$$

where  $e^{i\Phi_{\mathbf{k}}} = t_{\mathbf{k}}/|t_{\mathbf{k}}|$ . This corresponds to the  $T$ -matrix

$$T(\epsilon) = \frac{A_{uc}}{U_0^{-1} - \mathcal{G}_{AA}(\mathbf{0}, \epsilon)} \frac{\mathbb{1} + \Lambda_z \Sigma_z + \Lambda_y \Sigma_y - \Lambda_x \Sigma_x}{2}. \quad (41)$$

Using Eq. (37a), we arrive at Eq. (19).

To calculate the average cross-section, we note that in Eq. (32) only the first term survives, so the scattering is isotropic in space and completely mixes the valleys. The total out-scattering cross-section and the transport cross-section, averaged over the impurity positions, coincide and are given by

$$\overline{\sigma^{\text{out}}(\epsilon)} = \frac{\pi^2 v |\epsilon|/2}{\left( \frac{\pi v^2}{U_0 A_{uc}} + \epsilon \ln \frac{2v}{e\gamma r_0 |\epsilon|} \right)^2 + \left( \frac{\pi \epsilon}{2} \right)^2}. \quad (42)$$

This cross-section is plotted in Fig. 2 as a function of  $\epsilon$  for several values of  $U_0 = 1, 5, 10$  eV.

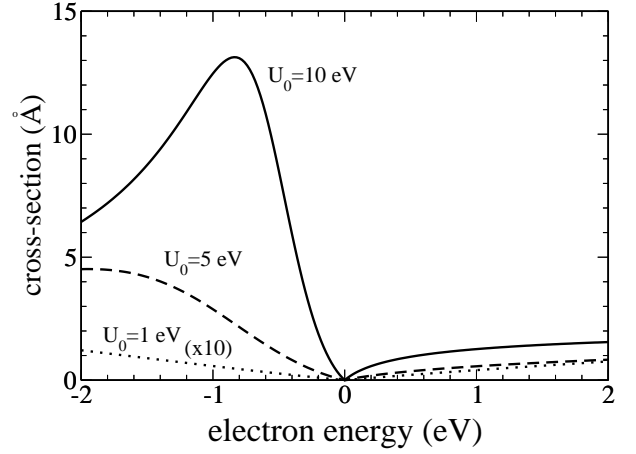


FIG. 2: The out-scattering cross-section (coinciding with the transport cross-section) for a one-site impurity of the strength  $U_0 = 1, 5, 10$  eV (dotted, dashed, and solid curve, respectively) as a function of the electron energy (in eV), as given by Eq. (42). The curve for  $U_0 = 1$  eV is multiplied by a factor of 10. The parameters of the model are  $v = 10^8$  cm/s = 6.58 Å,  $a = 1.42$  Å.

### C. Two-site impurity

Let us add a potential which mixes the two sites in the  $n_1 = n_2 = 0$  unit cell:

$$\mathcal{U} = \begin{pmatrix} U_0 & U_1 \\ U_1 & U_0 \end{pmatrix}. \quad (43)$$

We have chosen  $U_1$  to be real in order to preserve the  $A \leftrightarrow B$  symmetry. The self-consistent solution of the Lippmann-Schwinger equation gives

$$\mathcal{U}\Psi(\mathbf{0}) = [\mathcal{U}^{-1} - \mathcal{G}(\mathbf{0}, \epsilon)]^{-1} \Psi^{(0)}(\mathbf{0}) \equiv \mathcal{T}(\epsilon) \Psi^{(0)}(\mathbf{0}). \quad (44)$$

Comparing the resulting wave function with Eq. (17), we obtain

$$\begin{aligned} L = \frac{A_{uc}}{2\pi v} & \left[ \mathcal{T}(0) \frac{\mathbb{1} + \Lambda_z}{2} + \Sigma_y \mathcal{T}(0) \Sigma_y \frac{\mathbb{1} - \Lambda_z}{2} - \right. \\ & \left. - i\mathcal{T}(0) \Sigma_y \frac{\Lambda_x + i\Lambda_y}{2} + i\Sigma_y \mathcal{T}(0) \frac{\Lambda_x - i\Lambda_y}{2} \right]. \end{aligned} \quad (45)$$

For the potential of the form (43) the scattering lengths are obtained as [the matrix form of  $L$  is in agreement

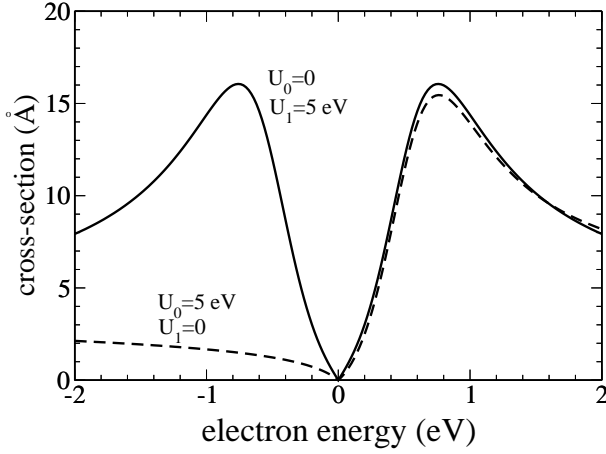


FIG. 3: The out-scattering cross-section for a two-site impurity with  $U_0 = 5$  eV,  $U_1 = 0$  (dashed curve), and  $U_0 = 0$ ,  $U_1 = 5$  eV (solid curve) as a function of the electron energy (in eV), as obtained from Eq. (47a). The parameters of the model are  $v = 10^8$  cm/s = 6.58 Å,  $a = 1.42$  Å.

with Eq. (25a)]:

$$\begin{aligned} \mathcal{T}(0) &= \frac{(U_0^2 - U_1^2)U_0}{U_0^2 + [U_1 + (a/2v)(U_0^2 - U_1^2)]^2} \mathbb{1} + \\ &+ \frac{(U_0^2 - U_1^2)(U_1 + (a/2v)(U_0^2 - U_1^2))}{U_0^2 - [U_1 + (a/2v)(U_0^2 - U_1^2)]^2} \Sigma_x \equiv \\ &\equiv \mathcal{T}_0 \mathbb{1} + \mathcal{T}_x \Sigma_x, \end{aligned} \quad (46a)$$

$$L = \frac{A_{uc} \mathcal{T}_0}{2\pi v} (\mathbb{1} + \Lambda_y \Sigma_y) + \frac{A_{uc} \mathcal{T}_x}{2\pi v} (\Lambda_z \Sigma_x + \Lambda_x \Sigma_z), \quad (46b)$$

$$l_{1,2} = \frac{A_{uc}}{\pi v} \frac{U_0 \pm U_1}{1 - (a/2v)(U_1 \pm U_0)}, \quad l_{3,4} = 0. \quad (46c)$$

The scattering lengths diverge when  $U_1 = 2v/a \pm U_0$ , in agreement with the results of Ref. 15.

Calculation of the  $T$ -matrix from Eq. (19) and its substitution into Eq. (32) gives the differential intravalley and intervalley cross-section (we set  $\varphi' = 0$ , as it depends only on  $\varphi - \varphi'$ ):

$$\frac{d\sigma_{\kappa\kappa'}}{d\varphi} = \frac{\pi v |\epsilon|}{8} \left[ |t_1|^2 + |t_2|^2 \pm \frac{|t_1 \pm t_2|^2}{2} \cos \varphi \right] \quad (47a)$$

$$t_{1,2}(\epsilon) = \frac{1}{v/l_{1,2} + \epsilon \ln[2v/(e\gamma r_0 |\epsilon|)] + i\pi\epsilon/2}. \quad (47b)$$

In Eq. (47a) the upper and lower sign is taken for the intravalley ( $\kappa = \kappa'$ ) and intervalley ( $\kappa \neq \kappa'$ ) scattering, respectively. The total out-scattering cross-section is plotted in Fig. 3 for the two cases of  $U_0 = 5$  eV,  $U_1 = 0$ , and  $U_0 = 0$ ,  $U_1 = 5$  eV.

## VII. CONCLUSIONS

In this paper we have studied scattering of low-energy electrons on a single neutral short-range impurity in

graphene within the framework of the 2D Dirac equation taking into account valley degeneracy. We have shown that for a general short-range scatterer the most important information needed to determine the cross-section is encoded in a  $4 \times 4$  matrix  $L$ , whose eigenvalues are the scattering lengths. Divergence of one or several scattering lengths occurs whenever the impurity has bound electronic states exactly at zero energy, which is accompanied by the singular behavior of the scattering cross-section as a function of the electronic energy. Quasi-bound states manifest themselves as resonances at finite energies, their width determined by the energy itself.

The matrix  $L$  can be obtained from the solution of a microscopic model for the impurity in graphene; only the zero-energy states need to be considered for this. As an example of a microscopic model we take the tight-binding model and calculate the scattering lengths for the diagonal one-site impurity potential and the two-site potential having both diagonal and off-diagonal components. We obtain that one of the scattering lengths indeed becomes much larger than the interatomic spacing for generic strong impurities (i. e., when impurity strength is of the order of the electronic bandwidth). This results in (i) a dramatic increase of the scattering cross-section and (ii) its strong energy dependence.

## VIII. ACKNOWLEDGEMENTS

The author thanks A. C. Ferrari, S. Piscanec, and F. Guinea for stimulating discussions.

## APPENDIX A: DIFFERENT REPRESENTATIONS OF THE STATE VECTOR

If one adopts a representation, different from (1) (let us denote the corresponding 4-columns by  $\tilde{\psi}$ ), the matrices  $\Sigma_i$ ,  $\Lambda_j$ ,  $i, j = x, y, z$ , instead of being simple Pauli matrices become some  $4 \times 4$  matrices. Their algebraic relations and symmetry properties, listed in Table II, remain the same. In fact, the convenient way to define these matrices for an arbitrary representation is to specify the irreducible representation of the  $C_{6v}$  group, the point group of graphene, according to which they transform. This is sufficient to fix their algebraic relations.<sup>34</sup> For example, the isospin matrices  $\Sigma_x, \Sigma_y$  are defined as the matrices, diagonal in the  $K, K'$  subspace, and transforming according to the  $E_1$  representation of  $C_{6v}$ .

As we have defined mutually commuting matrices  $\Sigma_i$  and  $\Lambda_j$ ,  $i, j = x, y, z$ , and have written the free electron hamiltonian in terms of the  $\Sigma$  matrices only, we must separate the degenerate valley subspace, defined as that invariant under the action of the  $\Sigma$  matrices. Since the basis vectors of representation (1) already have the necessary structure of the direct product, this representation is preferred for dealing with scattering problems. One can pass to it by choosing four basis vectors  $\tilde{\psi}_1, \dots, \tilde{\psi}_4$ ,

defined as eigenvectors of  $\Sigma_z$  and  $\Lambda_z$ :

$$\begin{aligned}\Sigma_z \tilde{\psi}_1 &= \Lambda_z \tilde{\psi}_1 = \tilde{\psi}_1, \\ -\Sigma_z \tilde{\psi}_2 &= \Lambda_z \tilde{\psi}_2 = \tilde{\psi}_2, \\ \Sigma_z \tilde{\psi}_3 &= -\Lambda_z \tilde{\psi}_3 = \tilde{\psi}_3, \\ -\Sigma_z \tilde{\psi}_4 &= -\Lambda_z \tilde{\psi}_4 = \tilde{\psi}_4.\end{aligned}\tag{A1}$$

Their relative phases are fixed by the requirement that the matrices  $\Sigma_i$  act as the Pauli matrices in the subspaces  $\{\tilde{\psi}_1, \tilde{\psi}_2\}$  and  $\{\tilde{\psi}_3, \tilde{\psi}_4\}$ , and  $\Lambda_i$  act as the Pauli matrices in the subspaces  $\{\tilde{\psi}_1, \tilde{\psi}_3\}$  and  $\{\tilde{\psi}_2, \tilde{\psi}_4\}$ . Thus, vectors  $\psi_1, \dots, \psi_4$  can be identified with the basis columns  $[1000]^T$ ,  $[0100]^T$ ,  $[0010]^T$ ,  $[0001]^T$  in representation (1), up to an overall phase. The two representations

are related by a unitary matrix  $U$ :  $\tilde{\psi} = U\psi$ .

The overall phase of the matrix  $U$  is fixed by requiring the proper form of the time reversal matrix. In the  $\tilde{\psi}$ -representation the unitary time reversal matrix  $\tilde{U}_t$  can be different from  $\Sigma_y \Lambda_y$ . Indeed, the matrices in the two representations are related by  $\tilde{U}_t = U U_t U^\dagger$  (while  $\Sigma_i$  and  $\Lambda_j$  are transformed by applying  $U$  and  $U^\dagger$ ), which is sensitive to the overall phase of  $U$ . However, the properties  $\tilde{U}_t^* \tilde{U}_t = \mathbb{1}$ , and  $\tilde{U}_t \Sigma_i^* \tilde{U}_t^\dagger = -\Sigma_i$ ,  $\tilde{U}_t \Lambda_i^* \tilde{U}_t^\dagger = -\Lambda_i$ ,  $i = x, y, z$ , do not depend on the representation. Applying these relations in the newly constructed representation, we obtain  $U_t = \Sigma_y \Lambda_y$  up to a phase; this phase is nullified by the appropriate choice of the phase of  $U$ .

---

\* Electronic address: basko@sissa.it

- <sup>1</sup> K. S. Novoselov, A. K. Geim, S. V. Morozov, D. Jiang, Y. Zhang, S. V. Dubonos, I. V. Grigorieva, and A. A. Firsov, *Science* **306**, 666 (2004).
- <sup>2</sup> J. C. Meyer, A. K. Geim, M. I. Katsnelson, K. S. Novoselov, T. J. Booth, and S. Roth, *Nature* **446**, 60 (2007).
- <sup>3</sup> S. Gilje, S. Han, M. Wang, K. L. Wang, and R. B. Kaner, *Nano Lett.* **7**, 3394 (2007).
- <sup>4</sup> C. Gómez-Navarro, R. T. Weitz, A. M. Bittner, M. Scolari, A. Mews, M. Burghard, and K. Kern, *Nano Lett.* **7**, 3499 (2007).
- <sup>5</sup> T. C. Echtermeyer, M. C. Lemme, M. Baus, B. N. Szafrank, A. K. Geim, and H. Kurz, *IEEE Electron Device Lett.* **29**, 952 (2008).
- <sup>6</sup> T. Ando and T. Nakanishi, *J. Phys. Soc. Jpn.* **67**, 1704 (1998).
- <sup>7</sup> H. J. Choi, J. Ihm, S. G. Louie, and M. L. Cohen, *Phys. Rev. Lett.* **84**, 2917 (2000).
- <sup>8</sup> H.-F. Song, J.-L. Zhu, and J.-J. Xiong, *Phys. Rev. B* **66**, 245421 (2002).
- <sup>9</sup> S.-H. Ke, H. U. Baranger, and W. Yang, *Phys. Rev. Lett.* **91**, 116803 (2003).
- <sup>10</sup> E. McCann and V. I. Fal'ko, *Phys. Rev. B* **71**, 085415 (2005).
- <sup>11</sup> V. M. Pereira, F. Guinea, J. M. B. Lopes dos Santos, N. M. R. Peres, and A. H. Castro Neto, *Phys. Rev. Lett.* **96**, 036801 (2006).
- <sup>12</sup> Yu. G. Pogorelov, arXiv:cond-mat/0603327.
- <sup>13</sup> N. M. R. Peres, F. Guinea, and A. H. Castro Neto, *Phys. Rev. B* **73**, 125411 (2006).
- <sup>14</sup> Yu. V. Skrypnik and V. M. Loktev, *Phys. Rev. B* **73**, 241402(R) (2006).
- <sup>15</sup> T. O. Wehling, A. V. Balatsky, M. I. Katsnelson, A. I. Lichtenstein, K. Scharnberg, and R. Wiesendanger, *Phys. Rev. B* **75**, 125425 (2007).
- <sup>16</sup> N. M. R. Peres, F. D. Klironomos, S.-W. Tsai, J. R. Santos, J. M. B. Lopes dos Santos, and A. H. Castro Neto, *Europhys. Lett.* **80**, 67007 (2007).
- <sup>17</sup> C. Bena, *Phys. Rev. Lett.* **100**, 076601 (2008).
- <sup>18</sup> O. V. Yazyev and L. Helm, *Phys. Rev. B* **75**, 125408 (2007).
- <sup>19</sup> V. V. Cheianov and V. I. Fal'ko, *Phys. Rev. Lett.* **97**,

- 226801 (2006).
- <sup>20</sup> N. H. Shon and T. Ando, *J. Phys. Soc. Jpn.* **67**, 2421 (1998).
- <sup>21</sup> H. Suzuura and T. Ando, *Phys. Rev. Lett.* **89**, 266603 (2002).
- <sup>22</sup> D. V. Khveshchenko, *Phys. Rev. Lett.* **97**, 036802 (2006).
- <sup>23</sup> E. McCann, K. Kechedzhi, V. I. Falko, H. Suzuura, T. Ando, and B. L. Altshuler, *Phys. Rev. Lett.* **97**, 146805 (2006).
- <sup>24</sup> K. Nomura and A. H. MacDonald, *Phys. Rev. Lett.* **98**, 076602 (2007).
- <sup>25</sup> K. Kechedzhi, O. Kashuba, and V. I. Falko, *Phys. Rev. B* **77**, 193403 (2008).
- <sup>26</sup> I. L. Aleiner and K. B. Efetov, *Phys. Rev. Lett.* **97**, 236801 (2006).
- <sup>27</sup> T. Stauber, N. M. R. Peres, and F. Guinea, *Phys. Rev. B* **76**, 205423 (2007).
- <sup>28</sup> P. M. Ostrovsky, I. V. Gornyi, and A. D. Mirlin, *Phys. Rev. B* **74**, 235443 (2006).
- <sup>29</sup> J. O. Sofo, A. S. Chaudhari, and G. D. Barber, *Phys. Rev. B* **75**, 153401 (2007).
- <sup>30</sup> R. G. Newton, *Scattering Theory of Waves and Particles*, (McGraw Hill, 1966).
- <sup>31</sup> D. P. DiVincenzo and E. J. Mele, *Phys. Rev. B* **29**, 1685 (1984).
- <sup>32</sup> M. I. Katsnelson and K. S. Novoselov, *Solid State Commun.* **143**, 3 (2007).
- <sup>33</sup> D. S. Novikov, *Phys. Rev. B* **76**, 245435 (2007).
- <sup>34</sup> D. M. Basko, *Phys. Rev. B* **78**, 125418 (2008).
- <sup>35</sup> D. M. Basko, *Phys. Rev. B* **76**, 081405(R) (2007).
- <sup>36</sup> K. Kechedzhi, E. McCann, V. I. Fal'ko, H. Suzuura, T. Ando and B. L. Altshuler, *Eur. Phys. J. Special Topics* **148**, 39 (2007).
- <sup>37</sup> L. D. Landau and E. M. Lifshitz, *Quantum mechanics*.
- <sup>38</sup> M. Lax, *Symmetry Principles in Solid State and Molecular Physics* (Dover, New York, 2001 or Wiley, New York, 1974).
- <sup>39</sup> For the states with negative energies,  $s = -1$ , the direction of the electron group velocity is opposite to that of momentum. Thus, for  $s = -1$  the scattered part of the wave function (6) represents an *incoming* flux of electrons. However, we prefer to work with the  $T$ -matrix for the chronologically ordered Green's function  $G(\mathbf{p}, \epsilon)$ , defined in Eq. (11),

rather than for the retarded Green's function  $G^R(\mathbf{p}, \epsilon)$ , the analytical continuation of  $G(\mathbf{p}, \epsilon)$  from the positive semi-axis of  $\epsilon$  through the upper complex half-plane of  $\epsilon$ . For this purpose we work with the solutions (6) which correspond to outgoing waves for electrons if  $s = 1$  and for holes if  $s = -1$ .

<sup>40</sup> Expression (19) can be compared to analogous expressions for the case of scalar particles with parabolic spectrum de-

termined by the mass  $m$  in the two- and three-dimensional cases [L. D. Landau and E. M. Lifshitz, *Quantum mechanics, non-relativistic theory*, (Pergamon Press, New York, 1977)]:  $T_{3D}(\epsilon) = (2\pi l/m)/(1 + ipl)$ ,  $l$  being the scattering length,  $p = \sqrt{2m\epsilon}$ , and  $T_{2D}(\epsilon) = (\pi/m)/[i\pi/2 - \ln(e^\gamma pr_0/2)]$ .